

Coupled CFD-HAM model sensitivity for material properties and boundary conditions

M. Van Belleghem, A. Willockx & M. De Paepe

Ghent University, Department of Flow, Heat and Combustion Mechanics, Ghent, Belgium

M. Steeman & A. Janssens

Ghent University, Department of Architecture and Urban Planning, Ghent, Belgium

ABSTRACT: Modelling heat, air and moisture transport in buildings accurately is of great importance when studying not only energy efficiency (for example heat losses and gains through the building envelope) but also damage mechanism (due to for example moisture accumulation or interstitial condensation). This is why a lot of effort has been put into the development of HAM models (Heat, Air and Moisture). Nevertheless these models still show some shortcomings. One of the mayor defects of classic HAM models is the poor air flow modelling. Often these models use transfer coefficients to model transport from air to porous material. To overcome this shortcoming, a coupled CFD-HAM approach is proposed. CFD (Computational Fluid Dynamics) is currently used to study air flow in and around buildings. By combining CFD with HAM, air flow around a porous material is simulated together with heat and moisture transport in the air and the porous material.

This paper shortly discusses a newly developed coupled CFD-HAM model. More specifically the sensitivity of the model to the necessary input data is investigated. Recent studies have shown that measured material property data can differ a lot when measured by different laboratories. Especially hygrothermal material properties like sorption isotherm and vapour permeability show large discrepancies. The objective of this paper is to investigate how changes in material properties affect the model outcome. Also the difference between modelling a building material as homogeneous or made up out of layers is studied.

From this sensitivity analysis it can be concluded that not all material properties are equally important. Variations in density, heat capacity and heat conductivity have almost no effect on the model. Hygrothermal properties like sorption isotherm and permeability on the other hand have a more severe impact, although this impact can still be considered acceptable in some cases. Nevertheless a high uncertainty on measured material properties combined with a high sensitivity for these parameters increase the uncertainty of the model outcome.

1 INTRODUCTION

Temperature and relative humidity are two important parameters for damage risk assessment of buildings. E.g. too high levels of indoor relative humidity can cause mould growth inside surfaces of the building envelope. When moisture migrates through the building envelope, interstitial condensation can occur which can lead to rot, deterioration of surface finishing materials or other damage phenomena. Even if humidity levels are kept low enough, damage can still occur due to too strong variations. E.g. paintings and artefacts can show cracks when exposed to fluctuating temperatures and humidity levels (Pavlogeorgatos, 2003). Having a good knowledge of the heat, air and moisture transport in a building is also of great importance for many other applications. Moisture buffering by hygroscopic materials levels out indoor relative humidity fluctua-

tions. This can reduce the energy use of HVAC systems (Osanyintola et al., 2006) and improve the perceived indoor air quality at the same time (Simonson et al., 2002). In literature some examples are found where the importance of knowing the relative humidity in the design stage of a HVAC system is highlighted (Steeman et al. 2009a, Woloszyn et al. 2009).

A new trend in Heat, Air and Moisture modelling (HAM) is the coupling of these models to CFD (Computational Fluid Dynamics).

However, these models still need proper input data like boundary conditions, initial conditions and material property data. Extensive databases for these material properties can be found in literature (Hens 1996, Hens 1991, Roels 2008), but recent studies revealed a large spread of some of these material properties when the same material was measured by different laboratories (Roels 2008, Roels et al.

2004). It is often not clear how this will affect the model outcome. Therefore this paper highlights the importance of a sensitivity analysis for newly developed coupled HAM models.

2 COUPLED CFD-HAM MODEL

Standard CFD packages do not include a HAM model to simulate the interaction with porous materials. Therefore a new model was added to an existing CFD package (Fluent®). This model is discussed more detailed in (Steeman et al., 2009b). In this paper only a short overview of the modelling approach is given.

Heat and moisture transfer in the air, porous material and at the interface is modelled in its full complexity. This makes the model very useful for the assessment of moisture related problems in microclimates.

A direct coupling approach is used. This implies that the computational domain encloses the air region as well as the porous material and only one solver is used. Nevertheless, for each region (porous material or air) a different set of equations has to be solved.

2.1 Heat and moisture transfer in the air

The air is modelled as an incompressible fluid. In this case the energy and moisture transport equations reduce to equations (1) and (2). Note that for the transported variables, temperature, T , is chosen for the energy equation and the mass fraction of water vapour, Y , for the moisture transport equation. The same transport variables are used in the transport equations for the porous material.

$$\frac{\partial}{\partial t}(\rho_{air}CT) + \nabla \cdot (\vec{v}\rho_{air}CT) = \nabla \cdot (\lambda_{air}\nabla(T) - (C_{vap} - C_{air})\vec{g}T) \quad (1)$$

$$\frac{\partial}{\partial t}(\rho_{air}Y) + \nabla \cdot (\rho_{air}\vec{v}Y) = \nabla \cdot (\rho_{air}D_{eff}\nabla(Y)) = -\nabla \cdot \vec{g} \quad (2)$$

with

$$C = YC_{vap} + (1 - Y)C_{air} \quad (3)$$

$$D_{eff} = D + D_{turb} \quad (4a)$$

$$D = 2.31 \times 10^{-5} \frac{101325}{P_{op}} \left(\frac{T}{273.16} \right)^{1.81} \quad (4b)$$

$$D_{turb} = \frac{\nu_{turb}}{Sc_{turb}} \quad (4c)$$

$$\lambda_{eff} = \lambda + \lambda_{turb} \quad (5a)$$

$$\lambda_{turb} = \rho C \frac{\nu_{turb}}{Pr_{turb}} \quad (5b)$$

In these equations ρ_{air} [kg/m³] is the density of the humid air, C_{vap} [J/kgK] is the specific heat capacity of water vapour, C_{air} [J/kgK] the specific heat capacity of air and C [J/kgK] the weighed average specific heat capacity according to equation (3), λ_{air} [W/mK] is the thermal conductivity of air and g [kg/m²s] the water vapour diffusion flux. D_{eff} [m²/s] is the effective diffusion coefficient of water vapour in air. D_{eff} is determined by equation (4). Here D is the molecular diffusion coefficient of water vapour in air which is only a property of the air water vapour mixture. This is given by equation (4b) where P_{op} represents the operating pressure. D_{turb} the turbulent diffusion coefficient and is a property of the mixture and the flow. The turbulent viscosity ν_{turb} [m²/s] is determined from the turbulence model of the considered flow and the turbulent Schmidt number is considered 0.7. λ_{eff} [W/mK] is the effective heat conductivity and is the sum of the molecular (λ) and turbulent conductivity (λ_{turb}) (equation (5)). The following values have been used for the different material properties: $C_{vap} = 1875.2$ J/kgK, $C_{air} = 1006.43$ J/kgK, $\lambda = 0.0257$ W/mK, $Pr_{turb} = 0.85$. The first term on the left hand side of each transport equation is the storage term, the second term represents the convective term; the right hand side represents the transport by diffusion.

2.2 Heat and moisture transfer in the porous material

For the porous material zone the following assumptions are made in the model:

- No air transfer occurs
- Liquid transfer is not dominant
- Moisture storage only depends on relative humidity
- The temperature remains below the boiling point
- There is no radiative transfer inside the porous material

The model is only valid in the hygroscopic range (RH < 98%). Here moisture transfer by equivalent moisture diffusion is dominant. This implies that the moisture transfer can be modelled by a single water vapour diffusion coefficient. Equations (6) and (7) describe the moisture transfer and the heat transfer in the porous material. Again temperature T and vapour mass fraction Y are used as the transported variables. Note how latent heat of vaporization L_{vap} appears in equation (7). Due to the capillary action of the porous material, part of the water vapour entering the porous material condenses (or when the porous material dries out, liquid water evaporates

from the pores). This phase change is accompanied by a latent heat effect.

$$\frac{dw}{dt} = -\nabla \cdot \vec{g} \Leftrightarrow \frac{\partial w}{\partial RH} \frac{\partial RH}{\partial Y} \frac{\partial Y}{\partial t} + \frac{\partial w}{\partial RH} \frac{\partial RH}{\partial T} \frac{\partial T}{\partial t} = \nabla \left(\rho \frac{D}{\mu} \nabla(Y) \right) \quad (6)$$

$$\begin{aligned} \frac{dE}{dt} &= \nabla \cdot (\lambda_{mat} \nabla(T) - ((C_{vap} - C_{air})T + L_{vap})\vec{g}) \Leftrightarrow \\ \rho_{mat} C \frac{\partial T}{\partial t} + C_{liq} T \frac{\partial w_{liq}}{\partial t} + (C_{vap} T + L_{vap}) \frac{\partial w_{vap}}{\partial t} &= \\ \nabla \cdot (\lambda_{mat} \nabla(T) - ((C_{vap} - C_{air})T + L_{vap})\vec{g}) & \end{aligned} \quad (7)$$

with

$$E = \rho_{mat} C_{mat} T + C_{liq} w_{liq} T + (C_{vap} T + L_{vap}) w_{vap} \quad (8)$$

$$C = C_{mat} + \frac{C_{liq} w_{liq}}{\rho_{mat}} + \frac{C_{vap} w_{vap}}{\rho_{mat}} \quad (9)$$

$$w_{liq} = \frac{\phi - \frac{w}{\rho_{vap}}}{\frac{1}{\rho_{liq}} - \frac{1}{\rho_{vap}}} \quad (10)$$

$$w_{liq} = \frac{\frac{w}{\rho_{liq}} - \phi}{\frac{1}{\rho_{liq}} - \frac{1}{\rho_{vap}}} \quad (11)$$

In equations (6) to (11) *mat* refers to material properties, *liq* stands for liquid water and *vap* for water vapour. In the material model described by equations (6) to (11) the following material properties have to be known: the sorption isotherm which states the relation between the equilibrium moisture content w [kg/m³] and the relative humidity RH [%], the vapour resistance factor μ [-] as function of the relative humidity, the thermal conductivity λ_{mat} [W/mK] of the porous material as function of the relative humidity, the dry density ρ_{mat} [kg/m³], the heat capacity C_{mat} [J/kgK] and the open porosity Φ [-].

3 REFERENCE CASE

In order to perform a sensitivity analysis on the coupled CFD-HAM model, a reference case was chosen first. The same case was used by Steeman et al. (2009b) to validate the coupled model. The case is based on an experimental setup discussed in detail by Talukdar et al. (2007). In this paragraph a short description of the test facility is given.

Figure 1 shows a schematic representation of the reference case setup. Only the section of interest is shown. The figure represents a part of a wind tunnel. Preconditioned air enters the section on the right hand side with a fully developed air profile. This air flows over a sample of porous material. Gypsum board was used for this investigation. Three gypsum

boards with a thickness of 12.5mm were stacked on top of each other. The gypsum boards have a length of 500mm and a width of 298mm. Only the top of the stack is in contact with the air duct, the other boundaries are assumed to be adiabatic. The cross section of the duct has a height of 20.5mm and a width of 298mm. Air enters the test setup at a constant temperature. The samples were preconditioned at a low relative humidity (30%) and constant temperature (23.3°C). Afterwards the relative humidity was changed to a higher value for 24 hours (RH=71.9%, T=23.8°C) and then lowered again for 24 hours (RH=29.6%, T=22.5°C). Thermocouples and RH sensors were placed at a depth of 12.5mm and 25mm to measure temperature and relative humidity in the hygroscopic material.

The average air velocity in the duct is 0.82 m/s which corresponds with a Reynolds number of 2000. The air is preconditioned before it enters the test section and an upstream developing section ensures a fully developed flow pattern. For the case of Re=2000 the airflow pattern is assumed to be laminar in accordance to Iskra et al. (2007).

A 2D structured grid was used, counting 33,800 rectangular cells. The grid is dense near the air material interface and gradually coarsens towards the bottom of the porous material and the centre of the duct. The grid dependency was investigated by using Richardson extrapolation (Roache, 1997). In order to reduce numerical diffusion a second order upwind scheme is used for the discretization of the convective terms. The PISO algorithm is used for the pressure-velocity coupling. To reduce the round-off errors, a double precision representation of real numbers is used.

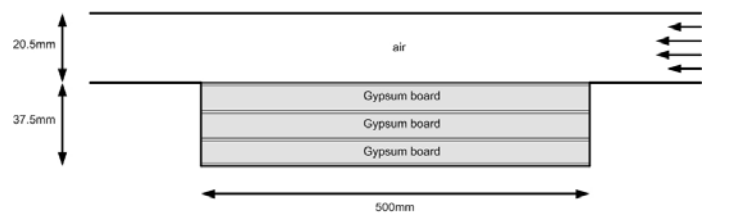


Figure 1. Reference case setup

4 MATERIAL PROPERTIES

The material properties used for the reference case were taken from IEA Annex 41 (Roels 2008). These properties are needed to solve equations (6) to (11). Report 2 of Annex 41 comprises an elaborate round robin test for some of these porous material properties. Samples of the same gypsum board were sent to different laboratories where the material properties were determined. Figure 2 and 3 show the average sorption isotherm and vapour resistance factor calculated from the data of Annex 41 (Roels 2008) together with the upper (+) and lower (-) measured

values. The round robin test performed in subtask 2 of this Annex revealed large discrepancies in the sorption isotherm and vapour resistance factor measured by 14 laboratories. Differences up to 20% are found. It can be expected that this will have an influence on the model outcome, since the accuracy of the solution is to a great extent determined by the accuracy of the input parameters.

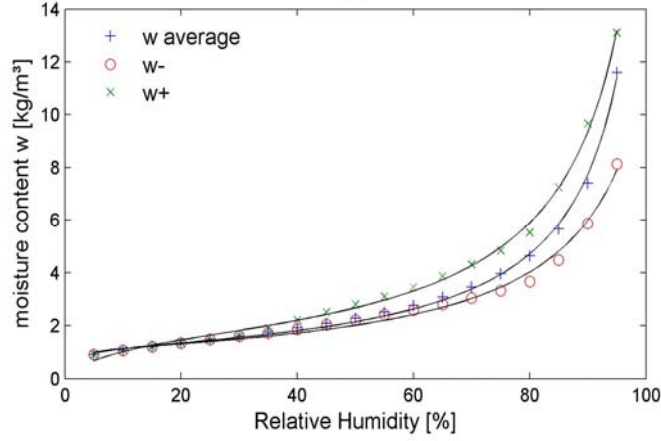


Figure 2. Sorption isotherm for gypsum board (data from Roels (2008))

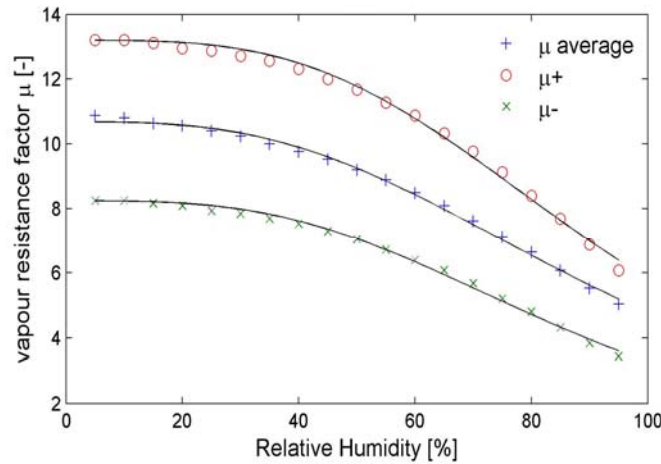


Figure 3. Vapour resistance factors for gypsum board (data from Roels (2008))

Table 1 lists five extra material properties of gypsum board used in the sensitivity analysis. For each property an upper and lower limit is determined, which corresponds with an increase or decrease of 5% of the original value. This is indicated in the table by Min(-5%) and Max(+5%). First, simulations are performed with the reference values. The output of these simulations is referred to as reference case. The sensitivity analysis is performed by changing one property at a time (One-at-a-Time analysis). Note that for this analysis the effect of density and porosity is not evaluated independently. In this study it is assumed that an increase of the open porosity by 5% would result in a decrease of the density by 5% and vice versa.

The properties listed in Table 1 are fairly easy to measure and are often measured quite accurate. This is why Report 2 of Annex 41 (Roels, 2008) only includes a sensitivity analysis for transfer coefficient, sorption isotherm and permeability. The influence of density, porosity, heat capacity and thermal conductivity was neglected. Nevertheless a measurement error (though limited) can always be expected, which still justifies a sensitivity analysis for these parameters.

The following analytical functions (12) and (13) are used for sorption isotherm and vapour resistance factor of gypsum board. The coefficients are determined by fitting the functions to experimental data.

Table 1. Material properties gypsum board

Material property	Reference value	-5%	+5%
Thickness d [m]	0.0125	-	-
Density ρ [kg/m³]	690	655.5	724.5
Open porosity Φ [-]	0.419	0.448	0.39
Thermal conductivity λ [W/mK]	0.198	0.188	0.208
Heat capacity C _{mat} [J/kgK]	840	798	882

$$w_a = \frac{RH}{aRH^2 + bRH + c} \quad (12)$$

$$\mu = \frac{\mu_0}{1 + aRH^n} \quad (13)$$

For each function a set of coefficients is given for the average curve fit, for the lower curve (-) and for the upper curve (+). No sensitivity analysis was performed on the desorption isotherm, so for this curve only one set of coefficients is given.

Table 2. Coefficient for sorption isotherm and vapour resistance factor of gypsum board corresponding to equation (12) and (13)

	+	Average	-
w _a			
a	-0.562516742	-0.81655	-0.8054748
b	0.560112656	0.85157	0.883480733
c	0.047583587	0.011176	0.007663124
μ			
μ ₀	13.2	10.68205	8.24
a	1.268102	1.229557	1.512357696
n	3.392995	2.983921	3.174273855

5 SENSITIVITY ANALYSIS

Studies of Roels (2008) and Roels et al. (2004) showed a large variability of measured material properties, which stresses the importance of a sensitivity analysis. The effect on numerical results for changes in the material properties will be studied in this section. In total five material properties are studied: dry density (combined with porosity), thermal

conductivity, heat capacity, sorption isotherm and moisture permeability, here represented as a water vapour resistance factor. The material properties of air are assumed constant in the model and are not investigated here. Their effect on the model is assumed negligible compared to the variability of the porous material properties. The same counts for the latent heat of vaporization which is again assumed constant in the model.

Temperature and relative humidity at a depth of 12.5mm and 25mm in the bed of gypsum board are simulated and a comparison between the different cases is made. In order to compare the results of the different simulations, Figure 4 proposes five parameters derived from a typical response of temperature and relative humidity inside gypsum board at a depth of 12.5mm to a step change in relative humidity (step change from 30%RH to 71.9%RH back to 29.6%RH). ΔRH_a indicates the magnitude of change in relative humidity after an absorption phase. ΔRH_d is the magnitude of change during a desorption phase. RH_{max} gives the maximum simulated relative humidity. T_{max} stands for the maximum simulated temperature and T_{min} the minimum temperature. A similar approach was used in Annex 41. For all simulations the boundary and inlet conditions are the same, so the effect of material properties can be revealed.

5.1 Density, thermal conductivity and heat capacity

The reference case is compared to the cases with different material properties. These simulations clearly show that changes of 5% in dry density, thermal conductivity and heat capacity have virtually no effect on the model outcome for both temperature and relative humidity. The same results were also found by Olutimayin et al. (2005). Olutimayin et al. measured and modelled heat and moisture transfer in cellulose insulation. He also performed a sensitivity analysis but changed the material properties by 10% instead of 5%. Still he concluded that the effect of thermal conductivity on the simulated temperature was less than 1% and could thus be neglected.

5.2 Sorption isotherm and vapour resistance factor

Simulations were performed for different sorption isotherms and vapour resistance factors corresponding with the curves shown on Figure 2 and 3. The results of these simulations are shown in Table 4.

Table 4 shows that an increase in sorption isotherm (w+) results in a decrease of the maximum relative humidity by 1.72% points and a decrease of the sorption isotherm (w-) results in an increase of the relative humidity by 0.94% points. These values are relatively low compared to the differences between the sorption isotherms.

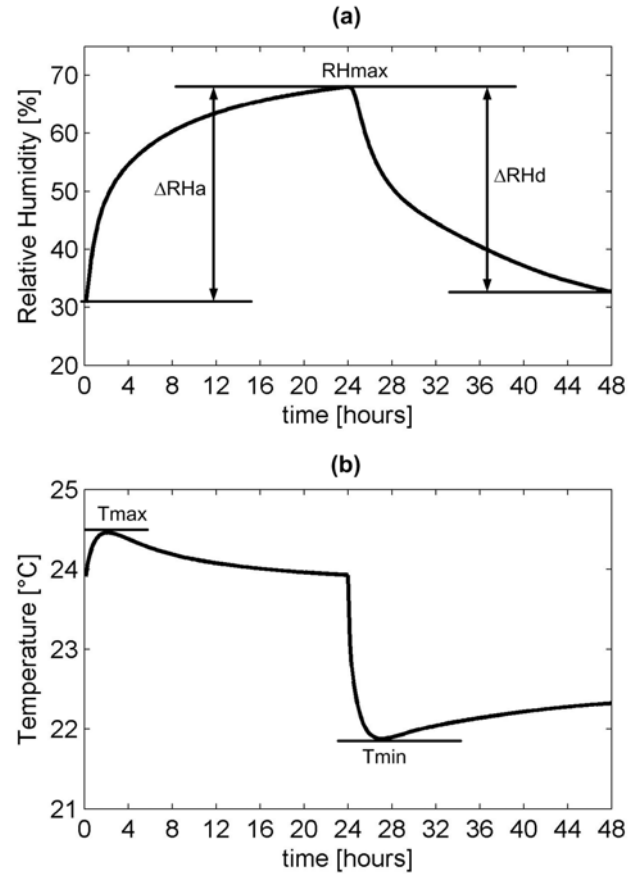


Figure 4. Typical response of the temperature (a) and relative humidity (b) in gypsum board at a depth of 12.5mm for a step change induced in the relative humidity of the surrounding air (29.6%RH-71.9%RH).

Changes in sorption isotherm also affect the simulated temperature. The temperature change due to latent heat effects is slightly smaller for a lower sorption isotherm and slightly larger for a higher sorption isotherm. These results correspond with what can be physically expected. An increased sorption isotherm will result in a higher moisture content and a higher specific moisture content ($\partial w / \partial RH$). This reduces the water vapour diffusion within the vapour phase and thus the relative humidity. Temperature change due to phase change increases because more vapour condenses during absorption and evaporates during desorption.

Talukdar et al. (2007) performed a similar study for spruce plywood and applied a $\pm 10\%$ deviation on each material property. He found similar results. Increasing the sorption isotherm with 10% resulted in a reduction of the relative humidity by 6% relative to the applied step change, which was 50%RH. A reduction of the sorption isotherm increased the relative humidity by 6% relative to the step change. He found that the difference between the measured and the simulated values for relative humidity were typically smaller than the fluctuations he found for different sorption isotherms. Thus he could conclude that the sorption isotherm he used for the modelling agreed well with reality.

Changing the vapour resistance factor by a higher or lower curve again changes the model outcome. Similar to the higher sorption isotherm, a higher vapour resistance factor results in a lower relative humidity during the absorption phase and a higher relative humidity during the desorption phase. The opposite counts for a lower vapour resistance factor. The effect is again more pronounced deeper in the material.

A higher vapour resistance factor corresponds with a lower vapour permeability. Thus it is more difficult for the water vapour to penetrate the porous material. This explains why a lower relative humidity is found during absorption and a higher relative humidity is found during desorption. Simultaneously the temperature change due to the latent heat effect is less pronounced for a higher vapour resistance factor and the other way around for a lower vapour resistance factor.

5.3 Modelling gypsum board as layered

Gypsum board is built up out of multiple layers but modelled as uniform which could effect the simulations. The gypsum board used in this study has a thickness of 12.5mm and consists out of three layers: a layer of finishing paper at both sides (thickness 0.5mm) and a layer of gypsum in between (thickness 11.5mm). Roels et al. (2006) measured the material properties for those layers separately. The sorption isotherms and vapour resistance factor for paper and gypsum are given by equations (15) and (16). The corresponding coefficients are listed in Table 3.

$$w = w_{sat} \left(1 + (-a\rho_w R_v T \ln(RH))^n \right)^{(1-n)/n} \quad (15)$$

$$\mu = \frac{1}{a + b \exp(cRH)} \quad (16)$$

Here ρ_w represents the water density (998.2 kg/m³) and R_v is the specific gas constant for water vapour (462 J/kgK).

Figure 10 shows some simulation results for relative humidity and temperature in the gypsum board for uniform modelling and layered modelling. The results differ from the reference case because a slightly different sorption isotherm and vapour resistance has been used: the curves used here were the ones measured by Roels et al. (2006) and correspond with the lower curves in Figure 2 and Figure 3. This explains why the predicted relative humidity is higher during absorption and lower during desorption. The difference in simulated relative humidity and temperature for the uniform and layered modelling is negligibly small, so modelling the gypsum board as layered has limited impact on the model outcome.

Table 3. Coefficients for the sorption isotherm and vapour resistance factor of finishing paper and gypsum

	Sorption isotherm		
	w_{sat}	a	n
Finishing paper	155	1.35e-6	1.48
Gypsum	130	50.7e-6	1.55
Uniform	130	24.8e-6	1.52
	Vapour resistance factor		
	a	b	c
Finishing paper	0.1	4.78e-3	4.10
gypsum	0.1	4.78e-3	4.10

Table 4 Simulation results for temperature and relative humidity at 12.5mm and 25mm in the gypsum board

	@12.5mm					@25mm				
	ΔRH_a [%]	ΔRH_d [%]	RHmax[%]	Tmax [°C]	Tmin [°C]	ΔRH_a [%]	ΔRH_d [%]	RHmax[%]	Tmax [°C]	Tmin [°C]
Reference case	38.02	35.31	68.02	24.46	21.88	35.64	30.83	65.64	24.54	21.81
$\rho+5\%$	38.02	35.32	68.02	24.44	21.89	35.64	30.84	65.64	24.53	21.82
$\rho-5\%$	38.02	35.31	68.02	24.47	21.86	35.64	30.83	65.64	24.56	21.79
$\lambda+5\%$	38.02	35.32	68.02	24.46	21.88	35.66	30.86	65.66	24.54	21.81
$\lambda-5\%$	38.01	35.30	68.01	24.46	21.88	35.62	30.80	65.62	24.55	21.80
$C_{mat}+5\%$	38.02	35.32	68.02	24.44	21.89	35.64	30.84	65.64	24.53	21.82
$C_{mat}-5\%$	38.02	35.31	68.02	24.48	21.86	35.64	30.83	65.64	24.56	21.79
Sorption isotherm +	36.30	31.27	66.30	24.57	21.83	33.03	24.32	63.03	24.66	21.78
Sorption isotherm -	38.96	37.26	68.96	24.41	21.91	37.07	33.96	67.07	24.50	21.83
$\mu+$	36.84	32.58	66.84	24.37	21.97	33.77	26.27	63.77	24.44	21.92
$\mu-$	39.18	37.97	69.18	24.57	21.75	37.51	35.45	67.51	24.68	21.65
Re=5000	38.21	35.66	68.21	24.34	21.97	35.85	31.24	65.85	24.43	21.90
Layered	40.18	39.11	70.18	24.51	21.83	39.12	37.08	69.12	24.62	21.72
Uniform	40.15	39.07	70.15	24.52	21.81	39.08	37.01	69.08	24.63	21.71

5.4 Air velocity and transfer coefficients

Simulation results shown up till now were all computed with laminar flow conditions. The average inlet velocity of 0.82m/s corresponds with $Re=2000$. Increasing the Reynolds number to 5000, and thus increasing the average velocity, results in a turbulent flow over the gypsum sample. Increasing the Reynolds number will also increase the transfer coefficients for heat and mass. Nevertheless, when analyzing Table 4 it is clear that this higher mass transfer coefficient has almost no effect on the response of the relative humidity inside the material. Mass transfer between the air and the porous materials is thus obviously dominated by the vapour diffusion resistance and not by the mass transfer coefficient. Same conclusions were also found in subtask 2 of Annex 41 (Roels, 2008) where a change of 10% in the mass transfer coefficient had no significant effect.

Increasing the heat transfer coefficient does lead to changes in the temperature response. The temperature change due to the latent heat effect is damped out due to the better heat transfer from the material to the air.

6 CONCLUSIONS

An extensive sensitivity analysis was performed on a recently developed coupled CFD-HAM model. This model uses CFD to calculate the indoor air distributions around a porous material and combines this with a HAM model to incorporate the heat and mass transfer between air and the porous material. By using a direct coupling method, no external data exchange between the two models is needed which increases the calculation speed of the model.

Data from a benchmark transient heat and mass transfer experiment performed during IEA Annex 41 were used as a reference case for the sensitivity analysis. The material data used for this case were the averaged values found in a round robin test also performed during IEA Annex 41. This test showed that large discrepancies could occur between material properties measured at different laboratories.

In this paper it is shown that the coupled CFD-HAM model is rather insensitive to deviations in most of the material properties. For density, heat capacity and thermal conductivity of the porous material no significant effect on simulated temperature and relative humidity was found. The impact of sorption isotherm and vapour resistance factor was more severe. These properties are often harder to measure, resulting in large uncertainties. Deviations up to 2%RH were found for the different isotherms and resistance factors. Changing both at the same time would lead to even larger deviations. These hygroscopic properties also have their impact on the calculated temperature although this is limited.

Finally, modelling gypsum board as layered had no impact on the results.

ACKNOWLEDGEMENT

The results presented in this paper have been obtained within the frame of the IWT SBO-050451 project heat, air and moisture performance engineering a whole building approach and the Flemish Institute for the Promotion and Innovation by Science and Technology in Flanders (IWT-SB/81322/Van Belleghem). Their financial support is gratefully acknowledged.

REFERENCES

- Pavlogeorgatos G. 2003. Environmental parameters in museums. *Building and Environment* 38, No. 12, 1457-1462.
- Osanyintola O.F. & Simonson C.J. 2006. Moisture buffering capacity of hygroscopic building materials: Experimental facilities and energy impact, *Energy and Buildings*, 38 No. 10, 1270-1282.
- Simonson C.J., Salonvaara M., Ojanen T. 2002. The effect of structures on indoor humidity - possibility to improve comfort and perceived air quality, *Indoor Air* 12 No. 4, 243-251
- Steeman M., Janssens A., De Paepe M. 2009a. Performance evaluation of indirect evaporative cooling using whole-building hygrothermal simulations, *Applied Thermal Engineering* 29 No.14-15, 2870-2875.
- Woloszyn M., Kalamees T., Olivier Abadie M., Steeman M., Sasic Kalagasidis A. 2009. The effect of combining a relative-humidity-sensitive ventilation system with the moisture-buffering capacity of materials on indoor climate and energy efficiency of buildings, *Building and Environment* 44 No. 3, 515-524.
- Hens H. 1996. *IEA Annex 24. Heat, Air and Moisture Transport, Final report, vol.1, Task 1: modelling*. International Energy Agency.
- Hens H. 1991. *IEA Annex 14: Condensation and Energy, vol.3: Catalogue of Material Properties*. International Energy Agency.
- Roels S. 2008. *IEA Annex 41. Whole Building Heat, Air and Moisture response. Subtask 2: Experimental Analysis of Moisture Buffering*. International Energy Agency.
- Roels S., Carmeliet J., Hens H., Adan O., Brocken H., Cerny R., Pavlik Z., Hall C., Kumaran K., Pel L., Plagge R. 2004. Interlaboratory Comparison of Hygric Properties of Porous Building Materials. *Journal of Thermal Envelope and Building Scienc* 27 No. 4, 307-325.
- Steeman H.-J., Van Belleghem M., Janssens A., De Paepe M. 2009b. Coupled simulation of heat and moisture transport in air and porous materials for the assessment of moisture related damage, *Building and Environment* 44 No.10, 2176-2184.
- Talukdar P., Olutmayin S.O., Osanyintola O.F., Simonson C.J. 2007. An experimental data set for benchmarking 1-D, transient heat and moisture transfer models of hygroscopic building materials. Part I: Experimental facility and material property data, *International Journal of Heat and Mass Transfer* 50 No. 23-24, 4527-4539.
- Iskra C.R., Simonson C.J. 2007. Convective mass transfer coefficient for a hydrodynamically developed airflow in a short rectangular duct, *International Journal of Heat and Mass Transfer* 50 No. 11-12, 2376-2393.

- Roache P.J. 1997. Quantification of uncertainty in computational fluid dynamics, *Annual Review of Fluid Mechanics* 29, 123-160.
- Olutimayin S.O. & Simonson C.J. 2005. Measuring and modeling vapor boundary layer growth during transient diffusion heat and moisture transfer in cellulose insulation. *International Journal of Heat and Mass Transfer* 48 No. 16, 3319-3330.
- Roels S, Janssen H, Carmeliet J, Diepens J, de Wit M. 2006. Hygric buffering capacities of uncoated and coated gypsum board. Research in Building Physics and Building Engineering - *Proceedings of the Third International Building Physics Conference*, Montreal, Canada.